

Size dependent torsional vibration of a rotationally restrained circular FG nanorod via strain gradient nonlocal elasticity

Büşra Uzun^{*1}, Ömer Civalek^{2,3a} and M. Özgür Yaylı^{1b}

¹Bursa Uludag University, Faculty of Engineering, Department of Civil Engineering, Görükle Campus, 16059, Bursa, Turkey

²Akdeniz University, Faculty of Engineering, Department of Civil Engineering, Antalya, Turkey

³Department of Medical Research, China Medical University Hospital, China Medical University, Taichung, Taiwan

(Received June 9, 2022, Revised October 25, 2023, Accepted December 5, 2023)

Abstract. Dynamical behaviors of one-dimensional (1D) nano-sized structures are of great importance in nanotechnology applications. Therefore, the torsional dynamic response of functionally graded nanorods which could be used to model the nano electromechanical systems or micro electromechanical systems with torsional motion about the center of twist is examined based on the theory of strain gradient nonlocal elasticity in this work. The mathematical background is constructed based on both strain gradient theory and Eringen's nonlocal elasticity theory. The equation of motions and boundary conditions of radially functionally graded nanorods are derived using Hamilton's principle and then transformed into the eigenvalue analysis by using Fourier sine series. A general coefficient matrix is obtained to assemble the Stokes' transformation. The case of a restrained functionally graded nanorod embedded in two elastic springs against torsional rotation is then deeply investigated. The effect of changing the functionally graded index, the stiffness of elastic boundary conditions, the length scale parameter and nonlocal parameter are investigated in detail.

Keywords: deformable boundaries; fourier sine series; functionally graded nanorod; strain gradient nonlocal; torsional vibration

1. Introduction

Recently, a lot of attention has been given to materials science. Developments in materials science and new types of materials produced provide significant benefits to other branches of science. Because the need for materials with better properties becomes evident day by day. One of these new types of materials is functionally graded materials (FGMs). Functionally graded (FG) materials are one of the relatively new types of composites and they have received attention recently. The mechanical properties of FG materials are smoothly changing from one point to another. This change may arise in one direction or in more directions. These composite materials in which the change takes place in one direction are called one-directional FG materials, while the materials in which the change occurs in two and three directions are called two- and three-directional functionally graded materials, respectively. Functionally graded materials come to the fore, especially in applications where working conditions are challenging. FGMs have a lot of potential in applications with harsh working circumstances, such as biomedical implants, spacecraft heat shields, plasma facings for fusion reactors, heat exchanger tubes and flywheels, among other things (Bohidar *et al.* 2014). In fact, the first application of the

FGM concept was its introduction as a thermal barrier material for a space shuttle in 1984 (Naebe and Shirvanimoghaddam 2016, Koizumi 1997).

The efficient mechanical properties of functionally graded materials compared to both homogeneous materials and classical (layered) composite materials have made them one of the focus of attention in recent times. Based on the various rod and beam theories, several studies were carried out to evaluate various responses of one-dimensional (1D) FG elements. Calim and Cuma (2021) examined the forced dynamic behavior of helical rods made of viscoelastic FG materials in conjunction with a thick beam theory. Shahba and Rajasekaran (2012) explored the critical buckling loads, axial frequencies and transverse frequencies in terms of non-dimensional forms for tapered beams made of axially FGMs. Ermiş (2021) presented the natural frequencies of elliptical, barrel and hyperboloidal helices consisting of axially FGM by using the mixed finite element method and also considered the warping effect into account in the study. Dynamic responses of axially FG Timoshenko beams embedded in a two-parameter elastic medium were presented by Calim (2020). Kiani and Eslami (2010) exploited the thermal stability behavior of thin beam composed of FG materials with power-law distribution. In addition to these studies, there are many papers (Madenci 2021, Ding and She 2021, Hadji *et al.* 2021, Tlidji *et al.* 2021, Shi *et al.* 2022) in the literature based on the different analyses of various structures made of FGMs. It should be noted here that other types of composites such as sandwich shell/plate, fibre-reinforced materials have also been used to model various structural elements (Li *et al.* 2022a, b, Dong *et al.* 2022).

*Corresponding author, Ph.D.,

E-mail: buzun@uludag.edu.tr

^a Ph.D., Professor, E-mail: civalek@yahoo.com

^b Ph.D., Professor, E-mail: ozguryayli@uludag.edu.tr

The scientific studies given above are on the response of macro-sized FGM rods and beams. Recently, nano and micro scale models of functionally graded materials have been solved via various non-classical elasticity theories. Torsional vibration analyses of functionally graded nanorods and nanotubes according to the nonlocal elasticity theory were performed by Zarezadeh *et al.* (2020), Civalek *et al.* (2022a), Shakhilavi *et al.* (2020). Torsional dynamic behavior of micro-/nanotubes and micro-/nanorods made of FGMs were investigated by Setoodeh and Zendehtdel Shahri (2016) and Civalek *et al.* (2022b), respectively. Noroozi *et al.* (2020) proposed the torsional frequencies of bi-directional FG nano-cone by using the nonlocal strain gradient (NLSG) theory (or strain gradient nonlocal theory) and applying the generalized differential quadrature method. Li and Hu (2016) explored the free dynamic frequencies and bending deflections of FG power-law nano-sized beams considering NLSG theory, thick beam theory and thin beam theory. Normalized bending deformations, maximum deflections, buckling loads forces and natural frequencies of axially FG beams were studied by Li *et al.* (2017) in the framework of the generalized differential quadrature method and NLSG theory. Ebrahimi *et al.* (2019) proposed a solution based on the Chebyshev–Ritz method for buckling and dynamic problems of FG materials which are depend on microstructure. Shen *et al.* (2016) studied the torsional vibration analysis of nano-scaled FG shaft via NLSG theory. Akgöz and Civalek (2014) presented the buckling loads in the dimensionless form of FG micro-sized beams for various beam theories, temperature change, gradient index and elastic foundation parameters. Also, the investigations based on a number of non-classical (higher-order) elasticity theories of nano-/micro-sized structures made of FGMs can be found in the studies presented by Ghandourah *et al.* (2021), Jalaei *et al.* (2022), Civalek *et al.* (2022c), Rahmani *et al.* (2020), Khoram *et al.* (2020), Norouzzadeh *et al.* (2020), Sahmani and Safaei (2019), Mahinzare *et al.* (2021), Uzun and Yaylı (2020), Alazwari *et al.* (2022). In addition to FGMs, studies (Devnath *et al.* 2022, Timesli 2021, Apuzzo *et al.* 2018, Xu *et al.* 2017, Numanoglu *et al.* 2022, Barretta *et al.* 2020, Gul and Aydogdu 2021, Arda and Aydogdu 2021, Lim *et al.* 2015, Civalek *et al.* 2020, Akgöz and Civalek 2013, Khosravi *et al.* 2020, Yaylı *et al.* 2021) examining the behavior of non-composite homogeneous tiny scale structures are generally employed in the scientific literature.

In the present theoretical work, utilizing the mixture of strain gradient elasticity and Eringen's nonlocal elasticity theories, an efficient solution method for static and free torsional vibration response of nanorods made of radially FG material with general boundary conditions is proposed. The functionally graded nanorod is considered slender and circular. Also, the mathematical model of functionally graded nanorod is established via massless torsional springs that restrain the FG nanorod. These massless torsional springs are used to present the deformable boundary conditions. Then, by applying the Stokes' transformation, a solution is obtained that saves re-solving according to changing boundary conditions of FGM nanorod. The solution obtained includes the springs at both ends of the

FG nanorod and other effects. In this single solution, the range of analysis is greatly extended by assigning the desired stiffnesses to the torsional spring parameters. Assigning high stiffnesses to these springs degenerates the springs to the clamped support, while assigning low stiffnesses degenerates the springs to the free end. As can be expected, numerous conditions in between these two cases can be easily analyzed with a single solution. In short, there is no need to resolve every time the boundary condition changes like other solution methods in the literature. With these features, the study gains originality and efficiency. Based on the best knowledge of the authors, the subject mentioned is presented for the first time in this study.

2. Introducing the theory of nonlocal strain gradient theory

In this section of the study, formulations in the theoretical background of the strain gradient nonlocal elasticity theory are derived. First, the governing equation of the torsional dynamic problem for the FG nano/micro sized rod is shown from the articles of Lim *et al.* (2015) and Shen *et al.* (2016). The displacement field components for a torsion rod are written as (Shen *et al.* 2016, Rao 2019):

$$u_x(x,t)=0 \quad (1)$$

$$u_y(x,t)=-z\Gamma(x,t) \quad (2)$$

$$u_z(x,t)=y\Gamma(x,t) \quad (3)$$

where, u_x , u_y and u_z represent the constituents of displacement field in cartesian coordinates (x , y and z). $\Gamma(x,t)$ denotes the rotational angular of the rod and t specifies the time. As it is known, the following relation can be written as:

$$\epsilon = \frac{1}{2}(\nabla u + (\nabla u)^T) \quad (4)$$

Here ϵ represents the strain and via Eqs. (1)-(4), the non-zero constituents for the torsional response of rod could be derived as follows (Shen *et al.* 2016):

$$\epsilon_{xy} = \epsilon_{yx} = -\frac{z}{2} \frac{\partial \Gamma(x,t)}{\partial x}, \quad \epsilon_{xz} = \epsilon_{zx} = -\frac{x}{2} \frac{\partial \Gamma(x,t)}{\partial x} \quad (5)$$

On the formulation background of the strain gradient nonlocal elasticity theory, the strain energy expression U is defined by (Lim *et al.* 2015, Shen *et al.* 2016):

$$\delta U = \frac{1}{2} \int_V (\sigma_{ij} \epsilon_{ij} + \sigma_{ijm}^{(1)} \epsilon_{ij,m}) dV \quad (6)$$

in the expression given in Eq. (6), V , A and L express the volume, cross-sectional area and length of the rod. Also, σ_{ij} embodies the nonlocal stress tensor and $\sigma_{ijm}^{(1)}$ denotes the higher-order nonlocal stress tensor. These stress tensors σ_{ij} and $\sigma_{ijm}^{(1)}$ are expressed in Eqs. (7) and (8), respectively (Lim *et al.* 2015):

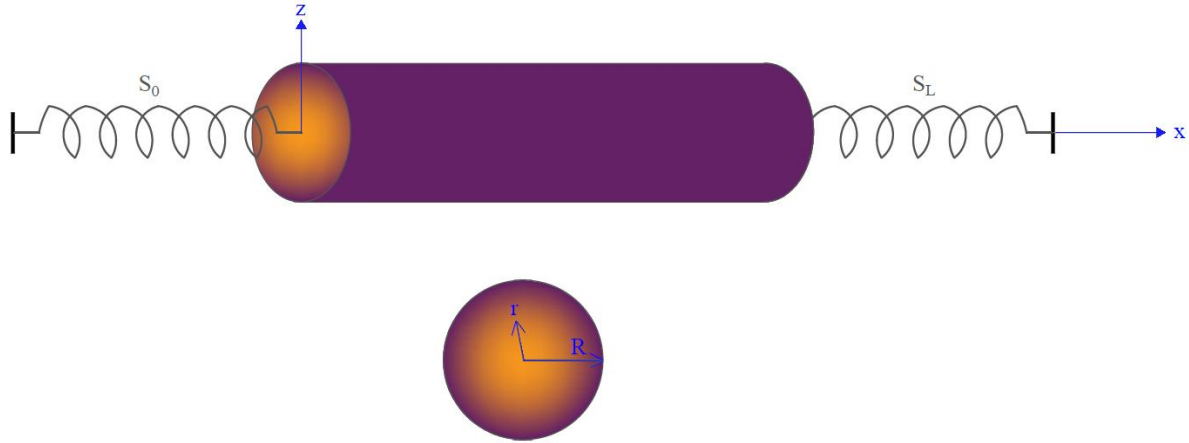


Fig. 1 Demonstration of a restrained nanorod made of radially FGM

$$\sigma_{ij} = C_{ijkl} \int_V \zeta_0(|x-x'|, \eta_0 a) \epsilon'_{kl} dV \quad (7)$$

$$\sigma_{ijm}^{(1)} = l^2 C_{ijkl} \int_V \zeta_1(|x-x'|, \eta_1 a) \epsilon'_{kl,m} dV \quad (8)$$

where, C_{ijkl} represents the classical elastic modulus tensor. l exemplifies the material size parameter (material length scale parameter) which is utilized for the investigating of the strain field. $\zeta_0(|x-x'|, \eta_0 a)$ and $\zeta_1(|x-x'|, \eta_1 a)$ are the kernel functions of nonlocal integral. Integrating the kernel functions in the integral here is quite difficult and elliptic integrals must be used. Also, $\eta_0 a$ and $\eta_1 a$ are used to investigate the stress field. The total stress field expression (τ_{ij}) in conjunction with NLSG theory is formulated as (Lim *et al.* 2015):

$$\tau_{ij} = \sigma_{ij} - \nabla \sigma_{ijm}^{(1)} \quad (9)$$

In Eq. (9), ∇ is the Laplacian formulation and defines the first derivative. Assuming $\eta_0 a = \eta_1 a = e_0 a$ and with the aid of Eq. (9), the constitutive law of strain gradient nonlocal theory can be derived as follows (Shen *et al.* 2016):

$$(1 - \mu \nabla^2) \tau_{ij} = (1 - l^2 \nabla^2) (\lambda \epsilon_{kk} \delta_{ij} + 2G(r) \epsilon_{ij}) \quad (10)$$

Here, $G(r)$ is the shear coefficient or modulus of the torsional response and $\mu = e_0 a^2$. Based on the previous relations, the first variation can be calculated as:

$$\begin{aligned} \delta U &= \int_V \left(2\sigma_{yx} \delta \epsilon_{yx} + 2\sigma_{yxx}^{(1)} \nabla \delta \epsilon_{yx} \right. \\ &\quad \left. + 2\sigma_{zx} \delta \epsilon_{zx} + 2\sigma_{zxx}^{(1)} \nabla \delta \epsilon_{zx} \right) dV \\ &\quad + \int_V (2t_{yx} \delta \epsilon_{yx} + 2t_{zx} \delta \epsilon_{zx}) dV \\ &= \int_V + \left[\int_A (2\sigma_{yxx}^{(1)} \delta \epsilon_{yx} + 2\sigma_{zxx}^{(1)} \delta \epsilon_{zx}) \right]_0^L \end{aligned} \quad (11)$$

Torsional vibration Eq. for nanorod can be derived by using Hamilton's technique. The formulation of the kinetic energy can be read as:

$$K = \int_V \rho(r) \left(\left(\frac{\partial u_x}{\partial t} \right)^2 + \left(\frac{\partial u_y}{\partial t} \right)^2 + \left(\frac{\partial u_z}{\partial t} \right)^2 \right) dV \quad (12)$$

$\rho(r)$ indicates the mass density of NLSG rod in the above Eq.. Now that the strain energy and kinetic energy expressions have been obtained, Hamilton's formulation can now be utilized. One can obtain the equilibrium Eq. of strain gradient with nonlocal elasticity as follows (Shen *et al.* 2016):

$$\psi_1 \frac{\partial^2 \Gamma(x, t)}{\partial x^2} - \frac{\partial T_x}{\partial x} = 0 \quad (13)$$

here, ψ_1 is represented the following expression:

$$\psi_1 = 2\pi \int_0^R \rho(r) r^3 dr \quad (14)$$

here, R and r are the radius value and radius direction of the FG nanorod, respectively. With the help of Eqs. (5) and (10), one can get:

$$T_x - \mu \frac{\partial^2 T_x}{\partial x^2} = \psi_2 \left(1 - l^2 \frac{\partial^2}{\partial x^2} \right) \frac{\partial \Gamma(x, t)}{\partial x} \quad (15)$$

In which, ψ_2 is the shear rigidity of the nanorod and it is defined by:

$$\psi_2 = 2\pi \int_0^R G(r) r^3 dr \quad (16)$$

By inserting Eq. (13) into Eq. (15), the below relation can be written:

$$T_x = \mu \psi_1 \frac{\partial^3 \Gamma(x, t)}{\partial x \partial t^2} + \psi_2 \left(1 - l^2 \frac{\partial^2}{\partial x^2} \right) \frac{\partial \Gamma(x, t)}{\partial x} \quad (17)$$

Considering Eqs. (13) and (17), the Eq. of torsional motion for strain gradient nonlocal FG nanorod is expressed as:

$$\begin{aligned} &\left[1 - (e_0 a)^2 \frac{\partial^2}{\partial x^2} \right] \psi_1 \frac{\partial^2 \Gamma(x, t)}{\partial t^2} \\ &- \psi_2 \left[1 - l^2 \frac{\partial^2}{\partial x^2} \right] \frac{\partial^2 \Gamma(x, t)}{\partial x^2} = 0 \end{aligned} \quad (18)$$

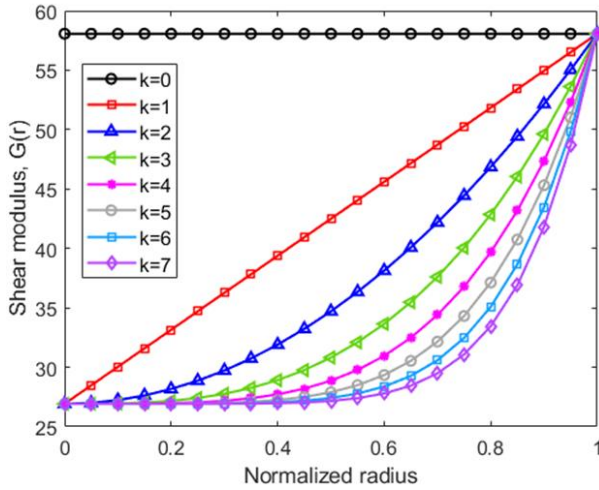


Fig. 2 Variation of shear modulus $G(r)$ versus normalized radius

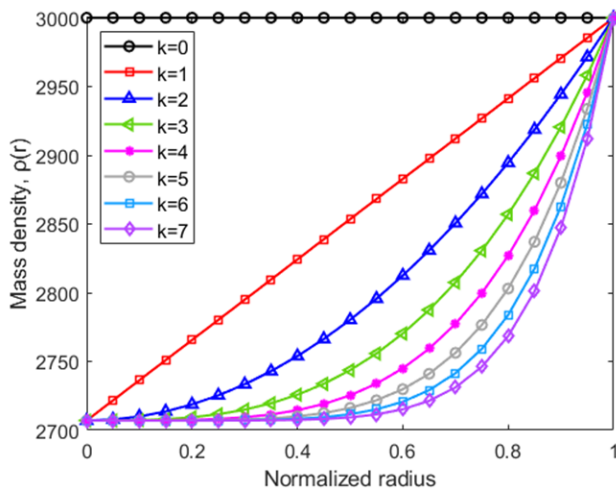


Fig. 3 Variation of mass density $\rho(r)$ versus normalized radius

3. Formulations of FG nanorod

Functionally graded materials are graded mechanical property materials and are used in important applications of various fields. In the present study, a nano-sized rod made of FG material with circular cross-section (Fig. 1) is considered. The functionally graded material have two different component in this study. In addition, mechanical characteristic of FG rod are vary in the radius direction of the cross-section. This means that in this study, which will examine the torsional vibration behavior, the shear modulus and mass density properties to be used in solving the problem change with a function that depends on the radius. The distribution function of material properties obeys the power-law model. The following relation expresses the change in the mechanic assumptions of the FG material according to the power law distribution in the direction of the radius. (Zhang *et al.* 2019):

$$\lambda(r) = (\lambda_s - \lambda_c) \left(\frac{r}{R}\right)^k + \lambda_c \quad (19)$$

In the above relation, $\lambda(r)$ represents the any effective material property of FG nano-sized rod in the radius direction (r). s and c given as subscripts represent the material specialities of the center and surface of the circular functionally graded nanorod, respectively. And lastly, k specifies the functionally gradient index. For the torsional problem based on NLSG theory, efficient shear modulus and density (mass) of the FG nanorod must be calculated. The efficient shear modulus $G(r)$ and density $\rho(r)$ are written according to Eq. (19) as follow:

$$G(r) = (G_s - G_c) \left(\frac{r}{R}\right)^k + G_c \quad (20)$$

$$\rho(r) = (\rho_s - \rho_c) \left(\frac{r}{R}\right)^k + \rho_c \quad (21)$$

With the help of the above relations, ψ_1 and ψ_2 are re-written by:

$$\psi_1 = 2\pi \int_0^R ((\rho_s - \rho_c) \left(\frac{r}{R}\right)^k + \rho_c) r^3 dr \quad (22)$$

$$\psi_2 = 2\pi \int_0^R ((G_s - G_c) \left(\frac{r}{R}\right)^k + G_c) r^3 dr \quad (23)$$

Also, the variation of the mechanical properties of FG NLSG rods according to the power-law distribution is investigated. For this purpose, Figs. (2) and (3) are plotted. In Fig. (2), variation of shear modulus of FG nanorod $G(r)$ is illustrated for various functionally gradient index ($k=0, 1, 2, 3, 4, 5, 6, 7$). Likely, variation of mass density of FG nanorod $\rho(r)$ is plotted for different functionally gradient index ($k=0, 1, 2, 3, 4, 5, 6, 7$) in Fig. (3). In these Figs., normalized frequency is defined as r/R and the material properties are: $G_c=26.92$ GPa, $G_s=58.07$ GPa, $\rho_c=2707$ kg/m³, $\rho_s=3000$ kg/m³. From these Figs., it can be easily understood that the center and surface of the nanorod have metal and ceramic properties, respectively. When we look at the effect of the functionally graded index k , we see that as k increases, the properties of the FG nanorod get closer to the metal.

4. Solution procedures

This section of the study aims to indicate the solution procedures of torsional vibration analysis based on the NLSG theory for a FG nanorod restrained with elastic torsional spring at both ends (see Fig. 1). Thank to the end of solution procedures, the torsional frequencies of FG nanorod with arbitrary boundary conditions can be calculated. First, separation of variables method formulated as below should be applied to Eq. (18):

$$\Gamma(x, t) = \phi(x)e^{i\omega t} \quad (24)$$

In which, $\phi(x)$ represents the rotation function, and ω denotes the torsional frequency of functionally graded nano-sized rod. Following Eq. is obtained by inserting Eq. (24) into the free torsional vibration expression in Eq. (18):

$$\psi_2 l^2 \frac{d^4 \phi(x)}{dx^4} - [\psi_2 - \mu \psi_1 \omega^2] \frac{d^2 \phi(x)}{dx^2} - \psi_1 \omega^2 \phi(x) = 0 \quad (25)$$

In this study, the rotation function specified by $\phi(x)$ is defined with three different regions as follows (Civalek *et al.* 2022a, b):

$$\phi(x) = \begin{cases} \phi_0 & x = 0 \\ \phi_L & x = L \\ \sum_{n=1}^{\infty} D_n \sin(\alpha_n x) & 0 < x < L \end{cases} \quad (26)$$

in which, D_n is the unknown Fourier coefficient and α_n is defined by:

$$\alpha_n = \frac{n\pi}{L} \quad (27)$$

This approach in this study allows to examine the torsional vibration behaviors of FG nanorod with general boundary conditions. It can easily be noticed that publications examining the torsional vibration of nanorods have focused on clamped at both ends, cantilever, and free-free boundary conditions (rigid boundary conditions). The solution method presented in this study solves any arbitrary boundary condition in addition to these three rigid boundary conditions. In this study, arbitrary boundary conditions are modeled with deformable torsional springs. Then, the Stokes' transform is employed to the governing Eq. of the free torsional problem and support conditions. D_n written in Eq. (39) may be defined as below:

$$D_n = \frac{2}{L} \int_0^L \phi(x) \sin(\alpha_n x) dx \quad (28)$$

If we write the first derivative of eq. (26), the following Eq. can be obtained:

$$\phi'(x) = \sum_{n=1}^{\infty} \alpha_n D_n \cos(\alpha_n x) \quad (29)$$

The above Eq. can be written by a cosine series as:

$$\phi'(x) = \frac{b_0}{L} + \sum_{n=1}^{\infty} b_n \cos(\alpha_n x) \quad (30)$$

The explicit forms via b_0 and b_n Fourier constants seen in eq. (30) are described as follows:

$$b_0 = \frac{2}{L} \int_0^L \phi'(x) dx = \frac{2}{L} (\phi_L - \phi_0) \quad (31)$$

$$b_n = \frac{2}{L} \int_0^L \phi'(x) \cos(\alpha_n x) dx \quad (n = 1, 2, \dots) \quad (32)$$

b_n coefficient can be calculated by integrating by parts of Eq. (32)

$$b_n = \frac{2}{L} [\phi(x) \cos(\alpha_n x)]_0^L + \frac{2}{L} \left(\alpha_n \int_0^L \phi(x) \sin(\alpha_n x) dx \right) \quad (33)$$

$$b_n = \frac{2}{L} ((-1)^n \phi_L - \phi_0) + \alpha_n D_n \quad (34)$$

4.1 Torsional static analysis of FG nanorod

The present solution procedure which is combination of Stokes' transformation and Fourier series is an efficient approach for FG torsion small-scale rods restrained with torsional elastic springs. The first-fourth derivatives of $\phi(x)$ are necessary for this study (Civalek *et al.* 2022a, b):

$$\frac{d\phi(x)}{dx} = \frac{\phi_L - \phi_0}{L} + \sum_{n=1}^{\infty} \cos(\alpha_n x) \left(\frac{2((-1)^n \phi_L - \phi_0)}{L} + \alpha_n D_n \right) \quad (35)$$

$$\frac{d^2 \phi(x)}{dx^2} = - \sum_{n=1}^{\infty} \alpha_n \sin(\alpha_n x) \left(\frac{2((-1)^n \phi_L - \phi_0)}{L} + \alpha_n D_n \right) \quad (36)$$

$$\frac{d^3 \phi(x)}{dx^3} = \frac{\phi_L'' - \phi_0''}{L} + \sum_{n=1}^{\infty} \cos(\alpha_n x) \left(\frac{2((-1)^n \phi_L'' - \phi_0'')}{L} - \alpha_n^2 \left(\frac{2((-1)^n \phi_L - \phi_0)}{L} + \alpha_n D_n \right) \right) \quad (37)$$

$$\frac{d^4 \phi(x)}{dx^4} = - \sum_{n=1}^{\infty} \alpha_n \sin(\alpha_n x) \left(\frac{2((-1)^n \phi_L'' - \phi_0'')}{L} - \alpha_n^2 \left(\frac{2((-1)^n \phi_L - \phi_0)}{L} + \alpha_n D_n \right) \right) \quad (38)$$

We can write Fourier coefficient D_n by using the above derivatives and the governing Eq. as follows:

$$D_n = -2\alpha_n \frac{\mu\beta_1 + \psi_2(l^2\beta_2 + \beta_3)}{L(\psi_1\omega^2\beta_4 - \psi_2\alpha_n^2\beta_5)} \quad (39)$$

In Eq. (39), β_i ($i=1, 2, 3, 4, 5$) are defined as:

$$\beta_1 = -\psi_1 \phi_0 \omega^2 + (-1)^n \psi_1 \omega^2 \phi_L \quad (40)$$

$$\beta_2 = -\phi_0'' - (-1)^n \phi_L \alpha_n^2 + (-1)^n \phi_L'' + \phi_0 \alpha_n^2 \quad (41)$$

$$\beta_3 = -(-1)^n \phi_L + \phi_0 \quad (42)$$

$$\beta_4 = \mu \alpha_n^2 + 1 \quad (43)$$

$$\beta_5 = l^2 \alpha_n^2 + 1 \quad (44)$$

With the help of Fourier coefficient D_n , the rotation function is rewritten as:

$$\phi(x) = \sum_{n=1}^{\infty} -2\alpha_n \frac{\mu\beta_1 + \psi_2(l^2\beta_2 + \beta_3)}{L(\psi_1\omega^2\beta_4 - \psi_2\alpha_n^2\beta_5)} \sin(\alpha_n x) \quad (45)$$

4.2 Torsional dynamic analysis of FG nanorod

The best knowledge of the authors, it is understood that there is no scientific paper examining the influences of deformable support conditions on the torsional free vibration response of FG nano-sized rods based nonlocal strain gradient theory. The aim of this study is to suggest a

general solution technique to calculate the torsional free vibration frequencies of the radially FG nanorod. The following relations including elastic spring parameters should be considered:

$$\mu\psi_1 \frac{\partial^3 \Gamma(0,t)}{\partial x \partial t^2} + \psi_2 \left(1 - l^2 \frac{\partial^2}{\partial x^2}\right) \frac{\partial \Gamma(0,t)}{\partial x} = S_0 \phi_0 \quad (46)$$

$$\mu\psi_1 \frac{\partial^3 \Gamma(L,t)}{\partial x \partial t^2} + \psi_2 \left(1 - l^2 \frac{\partial^2}{\partial x^2}\right) \frac{\partial \Gamma(L,t)}{\partial x} = S_L \phi_L \quad (47)$$

$$\frac{\partial^2 \phi_0''}{\partial x^2} = 0 \quad (48)$$

$$\frac{\partial^2 \phi_L''}{\partial x^2} = 0 \quad (49)$$

Here, Eqs. (46) and (48) satisfy the supporting condition at $x=0$, while expressions (47) and (49) satisfy the boundary relation at $x=L$. Also, S_0 and S_L seen in Eqs. (46) and (47) express the stiffnesses of the elastic springs at the ends of the FG nano-sized rod. We obtain two simultaneous homogeneous Eqs. substituting Eqs. (35), (37) and (39) into Eqs. (46) and (47)

$$\left(\begin{array}{c} -S_0 + \frac{\mu\psi_1\omega^2}{L} - \frac{\psi_2}{L} \\ 2L\psi_1\omega^2(\mu\psi_1\omega^2L^2 - \psi_2(L^2 + \pi^2n^2l^2)) \\ -\psi_2(L^2 + \pi^2n^2l^2) \\ \frac{L^2\psi_1\omega^2(L^2 + \mu\pi^2n^2)}{-\pi^2n^2\psi_2(L^2 + \pi^2n^2l^2)} \end{array} \right) \phi_0 + \sum_{n=1}^{\infty} \left(\begin{array}{c} -\frac{\mu\psi_1\omega^2}{L} + \frac{\psi_2}{L} \\ 2(-1)^n L\psi_1\omega^2(\mu\psi_1\omega^2L^2 - \psi_2(L^2 + \pi^2n^2l^2)) \\ -\psi_2(L^2 + \pi^2n^2l^2) \\ \frac{L^2\psi_1\omega^2(L^2 + \mu\pi^2n^2)}{-\pi^2n^2\psi_2(L^2 + \pi^2n^2l^2)} \end{array} \right) \phi_L = 0 \quad (50)$$

$$\left(\begin{array}{c} -\frac{\mu\psi_1\omega^2}{L} + \frac{\psi_2}{L} \\ 2(-1)^n L\psi_1\omega^2(\mu\psi_1\omega^2L^2 - \psi_2(L^2 + \pi^2n^2l^2)) \\ -\psi_2(L^2 + \pi^2n^2l^2) \\ \frac{L^2\psi_1\omega^2(L^2 + \mu\pi^2n^2)}{-\pi^2n^2\psi_2(L^2 + \pi^2n^2l^2)} \end{array} \right) \phi_0 + \sum_{n=1}^{\infty} \left(\begin{array}{c} -S_L + \frac{\mu\psi_1\omega^2}{L} - \frac{\psi_2}{L} \\ 2L\psi_1\omega^2(\mu\psi_1\omega^2L^2 - \psi_2(L^2 + \pi^2n^2l^2)) \\ -\psi_2(L^2 + \pi^2n^2l^2) \\ \frac{L^2\psi_1\omega^2(L^2 + \mu\pi^2n^2)}{-\pi^2n^2\psi_2(L^2 + \pi^2n^2l^2)} \end{array} \right) \phi_L = 0 \quad (51)$$

Thanks to Eqs. (50) and (51), an eigenvalue problem involving nonlocal effect, strain gradient effect and the torsional spring restraints may be constructed as:

$$\begin{bmatrix} \zeta_{11} & \zeta_{12} \\ \zeta_{21} & \zeta_{22} \end{bmatrix} \begin{bmatrix} \phi_0 \\ \phi_L \end{bmatrix} = 0 \quad (52)$$

In this work, an effective solution technique based on the Fourier series including a mathematical transformation

known as Stokes' transformation and a combined procedure is applied to overcome the angular rotation around the center of twist and torsion restraints at both ends of the FG nano-sized rod. Thanks to this presented solution approach, arbitrary boundaries for the functionally graded nanorod can be solved. Also, non-deformable support conditions may be investigated by setting appropriate stiffness values to the torsional springs of FG nanorod. For instance, it would be appropriate to select $S_0 = 0$ and $S_L = 0$ to calculate free boundary conditions at $x=0$ and $x=L$ of the FG nanorod. Otherwise, at $x=0$ and $x=L$, the clamped boundary conditions may be achieved with $S_0 = \infty$ and $S_L = \infty$. The free torsional vibration frequencies of the FG nonlocal strain gradient rod are obtained by letting the determinant of the coefficient matrix to zero after setting the torsional spring stiffnesses.

$$\begin{vmatrix} N_{11} & N_{12} \\ N_{21} & N_{22} \end{vmatrix} = 0 \quad (53)$$

here,

$$N_{11} = -S_0 + \frac{\mu\psi_1\omega^2}{L} - \frac{\psi_2}{L} + \sum_{n=1}^{\infty} \frac{2L\psi_1\omega^2(\mu\psi_1\omega^2L^2 - \psi_2(L^2 + \pi^2n^2l^2))}{L^2\psi_1\omega^2(L^2 + \mu\pi^2n^2) - \pi^2n^2\psi_2(L^2 + \pi^2n^2l^2)} \quad (54)$$

$$N_{12} = -\frac{\mu\psi_1\omega^2}{L} + \frac{\psi_2}{L} - \sum_{n=1}^{\infty} \frac{2(-1)^n L\psi_1\omega^2(\mu\psi_1\omega^2L^2 - \psi_2(L^2 + \pi^2n^2l^2))}{L^2\psi_1\omega^2(L^2 + \mu\pi^2n^2) - \pi^2n^2\psi_2(L^2 + \pi^2n^2l^2)} \quad (55)$$

$$N_{21} = -\frac{\mu\psi_1\omega^2}{L} + \frac{\psi_2}{L} - \sum_{n=1}^{\infty} \frac{2(-1)^n L\psi_1\omega^2(\mu\psi_1\omega^2L^2 - \psi_2(L^2 + \pi^2n^2l^2))}{L^2\psi_1\omega^2(L^2 + \mu\pi^2n^2) - \pi^2n^2\psi_2(L^2 + \pi^2n^2l^2)} \quad (56)$$

$$N_{22} = -S_0 + \frac{\mu\psi_1\omega^2}{L} - \frac{\psi_2}{L} + \sum_{n=1}^{\infty} \frac{2L\psi_1\omega^2(\mu\psi_1\omega^2L^2 - \psi_2(L^2 + \pi^2n^2l^2))}{L^2\psi_1\omega^2(L^2 + \mu\pi^2n^2) - \pi^2n^2\psi_2(L^2 + \pi^2n^2l^2)} \quad (57)$$

In this section, static and dynamic formulations of FG nanorod via the NLSG are derived. For dynamic analysis, a coefficients matrix is obtained to calculate the free torsional frequencies of FG nanorod affected by nonlocality and strain gradient. The obtained coefficient matrix includes μ , l , functionally graded index k and the torsional spring stiffnesses S_0 and S_L . It should be highlighted here that a number of prominent points about the coefficients matrix. If one sets l to zero in the coefficients matrix and realizes the dynamic analysis, one obtains the free torsional vibration frequencies of a FG nonlocal rod. Also, if one sets the μ to zero in the coefficients matrix and performs the dynamic analysis, one calculates the free torsional vibration frequencies of a FG strain gradient rod. And lastly, if both μ and l are set to zero and solution is realized, the free torsional vibration frequencies of functionally graded classical rod are gained. It is also important to note here that the presented eigenvalue solution does not only give the

torsional vibrational frequencies of nanorods made of FG materials. Given appropriate values for the functionally gradient index, the solutions are reduced to the frequencies of homogeneous nanorods.

5. Validations and numerical examples

In this section of the study, applications of the presented method are realized for functionally graded nano-sized rod. Examined NLSG rod made of FG material is considered with circular cross-section. A number of applications are shown on the change of the mechanical properties of the FG nonlocal strain gradient rod formed from ceramic and metal components. This change occurs in the direction of the functionally graded nanorod's radius. In this study, center of the FGM nanorod is composed of metal, while surface of the FGM nanorod is composed of ceramic. The shear modulus and mass density of the components in the center and surface are: $G_c=26.92$ GPa, $G_s=58.07$ GPa, $\rho_c=2707$ kg/m³, $\rho_s=3000$ kg/m³. It should be noted here that the given shear modulus values are calculated using the relation $G = E/(2(1 + \nu))$ between shear modulus and Young's modulus. The Poisson's ratios of components in the center and surface of the FG nanorod are equal and is 0.3. Also, the Young's module of components in the center and surface of the functionally graded nanorod are 70 GPa and 151 GPa, respectively. The radius and length of functionally graded nonlocal strain gradient rod are selected as $R=2$ nm and $L=20$ nm for all numerical applications.

5.1 Validation study

In this section of the study, validation of the shown method is presented. Li *et al.* (2016) proposed the free axial frequency Eqs. of different boundary conditions as below:

$$\Omega = \frac{m\pi}{L} \sqrt{\frac{E(L^2 + l^2 m^2 \pi^2)}{\rho(L^2 + \mu m^2 \pi^2)}} \quad (58)$$

for clamped-clamped nanorod and (Li *et al.* 2016)

$$\Omega = \frac{(2m-1)\pi}{2L} \sqrt{\frac{E(4L^2 + l^2 m^2 \pi^2)}{\rho(4L^2 + \mu m^2 \pi^2)}} \quad (59)$$

for clamped-free nanorod. In Eqs. (58) and (59), m defines the mode number and Ω denotes the angular frequency for axial vibration. In the above Eqs., if we set $E=G$, we can obtain the free torsional frequency Eqs. as follows:

$$\omega = \frac{m\pi}{L} \sqrt{\frac{G(L^2 + l^2 m^2 \pi^2)}{\rho(L^2 + \mu m^2 \pi^2)}} \quad (60)$$

for clamped-clamped nanorod and

$$\omega = \frac{(2m-1)\pi}{2L} \sqrt{\frac{G(4L^2 + l^2 m^2 \pi^2)}{\rho(4L^2 + \mu m^2 \pi^2)}} \quad (61)$$

for clamped-free nanorod. The above relations are belong to homogeneous nanorods. Shen *et al.* (2016) have introduced the following relation for FG strain gradient nonlocal nanorods at clamped-clamped condition:

Table 1 Comparison studies for torsional frequencies (10^{11} rad/s) of homogeneous nanorod for various small scale parameter ($L=20$ nm, mode 1)

clamped-clamped			
$\sqrt{\mu}=0.5$ nm	$l=0.1$ nm	$l=0.8$ nm	$l=1.8$ nm
Ref. (Eqs. 60 and 62)	6.89	6.94	7.16
Present study ($S_0 = S_L = \infty$)	6.89	6.94	7.16
clamped-free			
$\sqrt{\mu}=1$ nm	$l=0.1$ nm	$l=0.8$ nm	$l=1.8$ nm
Ref. (Eq. 61)	3.45	3.46	3.49
Present study ($S_0 = \infty$ & $S_L = 0$)	3.45	3.46	3.49

$$\omega = \frac{m\pi}{L} \sqrt{\frac{\psi_2(L^2 + l^2 m^2 \pi^2)}{\psi_1(L^2 + \mu m^2 \pi^2)}} \quad (62)$$

To compare the frequency values and show the validation of the study, we achieve two different comparison study. First, we compare the torsional frequency values of clamped-clamped homogeneous nanorods. For this, we use Eq. (53) and the parameters $k=0$, $S_0=\infty$ and $S_L=\infty$. To achieve the homogeneous nanorod properties, k is selected as zero. In addition, $S_0=\infty$ and $S_L=\infty$ are selected to intercept clamped-clamped boundary condition. Secondly, by using Eq. (53) again, torsional vibration frequencies are compared for $k=0$. For the second comparison study, $S_0=\infty$ and $S_L=0$ are selected to ensure clamped-free boundary condition. A very good agreement is achieved in both comparison studies. In addition this agreement is demonstrate via Table 1. It should also be noted here that when $S_0 = \infty$ or $S_L = \infty$ is written throughout the study, the dimensionless spring stiffness \bar{S}_0 or \bar{S}_L is actually taken as 10^{16} which is close to infinity in the calculations. On the other hand, when $S_0 = 0$ or $S_L = 0$, \bar{S}_0 or \bar{S}_L , which is actually the dimensionless spring stiffness in the calculations, is taken as 10^{-16} , which is a value close to zero. These dimensionless spring stiffnesses are calculated as follows:

$$\bar{S}_0 = \frac{S_0 L}{G_s J} \quad (63)$$

$$\bar{S}_L = \frac{S_L L}{G_s J} \quad (64)$$

Here, J is calculated as follows:

$$J = \frac{\pi R^4}{2} \quad (65)$$

For the above comparison and the analyses, it should be noted that the number of terms for clamped-clamped is 20 ($n=20$), while the number of terms for clamped-free is 250 ($n=250$). The appropriate number of terms varies based on the boundary condition to be investigated. The authors use a low number of terms for hard springs and a high number of terms for soft springs with reference to the previous studies presented by the authors with Fourier series and Stokes

Table 2 Variation of torsional frequencies (10^{11} rad/s) of FG nanorod with hard-hard springs for various functionally gradient index ($\sqrt{\mu} = 0.5$ nm and $l = 0.3$ nm)

mode number	functionally gradient index (k)							
	k=0	k=1	k=2	k=3	k=4	k=5	k=6	k=7
1	6.9	6.58	6.35	6.18	6.05	5.94	5.85	5.78
2	13.72	13.09	12.64	12.3	12.03	11.82	11.64	11.49
3	20.38	19.45	18.78	18.27	17.88	17.56	17.3	17.08
4	26.84	25.61	24.73	24.06	23.54	23.12	22.78	22.49
5	33.05	31.53	30.45	29.63	28.99	28.47	28.05	27.69
6	38.98	37.2	35.91	34.95	34.19	33.58	33.09	32.67

Table 3 Variation of torsional frequencies (10^{11} rad/s) of FG nanorod with hard-soft springs for various functionally gradient index ($\sqrt{\mu} = 0.5$ nm and $l = 0.3$ nm)

mode number	functionally gradient index (k)							
	k=0	k=1	k=2	k=3	k=4	k=5	k=6	k=7
1	3.45	3.3	3.18	3.1	3.03	2.98	2.93	2.89
2	10.32	9.85	9.51	9.25	9.05	8.89	8.76	8.65
3	17.07	16.29	15.73	15.31	14.97	14.71	14.49	14.31
4	23.64	22.56	21.78	21.19	20.74	20.37	20.06	19.81
5	29.98	28.60	27.62	26.87	26.29	25.83	25.44	25.12
6	36.05	34.40	33.21	32.32	31.62	31.06	30.6	30.21

Table 4 Variation of torsional frequencies (10^{11} rad/s) of FG nanorod with hard-hard springs for various functionally gradient index ($\sqrt{\mu} = 1.0$ nm and $l = 0.8$ nm)

mode number	functionally gradient index (k)							
	k=0	k=1	k=2	k=3	k=4	k=5	k=6	k=7
1	6.88	6.57	6.34	6.16	6.04	5.93	5.84	5.77
2	13.6	12.97	12.53	12.19	11.93	11.71	11.54	11.39
3	20.0	19.13	18.47	17.97	17.58	17.27	17.01	16.8
4	26.2	25.00	24.14	23.49	22.98	22.57	22.24	21.96
5	32.1	30.63	29.57	28.77	28.15	27.65	27.24	26.9
6	37.79	36.06	34.82	33.88	33.15	32.56	32.08	31.67

Table 5 Variation of torsional frequencies (10^{11} rad/s) of FG nanorod with hard-soft for various functionally gradient index ($\sqrt{\mu} = 1.0$ nm and $l = 0.8$ nm)

mode number	functionally gradient index (k)							
	k=0	k=1	k=2	k=3	k=4	k=5	k=6	k=7
1	3.45	3.29	3.18	3.09	3.03	2.97	2.93	2.89
2	10.27	9.80	9.46	9.21	9.00	8.85	8.72	8.61
3	16.86	16.09	15.53	15.11	14.79	14.52	14.31	14.13
4	23.16	22.10	21.33	20.76	20.31	19.95	19.65	19.41
5	29.18	27.84	26.88	26.16	25.59	25.14	24.76	24.45
6	34.97	33.36	32.21	31.35	30.70	30.12	29.68	29.30

transform. As it is known, most of the studies in the literature are based on idealised clamped or free end for rod

type elements. In this study, however, non-ideal and deformable boundary conditions more suitable for real life applications are used. The purpose of the study is already original. Infinitely rigid or infinitely free supports are not possible in practice. However, the majority of the studies are carried out in this way because functions that fit the analytical solution functions (Fourier sine or cosine series) can be selected away from the application. In other words, since the solution is done in this way, the selection is also rigid. In this study, whatever the boundary conditions are, a mathematical function (Stokes' transform) is forced to satisfy the boundary conditions.

5.2 Numerical examples

In Table 2, an example is given to investigate the impact of functionally gradient index on the torsional frequencies of radially FG nanorod with hard torsional springs ($S_0=S_L=\infty$). In the study presented in Table 2, functionally gradient index changes from 0 to 7 at intervals of 1 and the first six mode torsional frequencies are examined. In Table 3, the frequencies with the same functionally gradient index values as Table 2 are obtained for the FG nonlocal strain gradient rod with hard spring ($S_0=\infty$) at first end and soft spring ($S_L=0$) other end. The nonlocal parameter and material length scale parameter are selected as $\sqrt{\mu} = 0.5$ nm and $l = 0.3$ nm, respectively for the first two tables.

The different values of the k are used in Table 4 to investigate the impact of the functionally gradient index on the first six torsional frequencies of FG nanorods with hard torsional springs ($S_0=S_L=\infty$). The index varies from 0 to 7 same as the all tables. Table 5 shows the torsional frequencies for the radially functionally graded nonlocal strain gradient rod with hard spring ($S_0=\infty$) at one end and soft spring ($S_L=0$) at the other end, with the same functionally graded index values as the all tables. The nonlocal parameter is set to $\sqrt{\mu} = 1$ nm, while the material length scale parameter is set to $l = 0.8$ nm for the last two tables.

For more good understanding, the torsional frequency values in Tables 2-5 are illustrated via a number of Figures. Figs. (4) and (5) show the variation of torsional frequencies in terms of rad/s for the first six modes versus functionally gradient index. Fig. (4) demonstrates the frequencies of the FG nonlocal strain gradient rod with hard torsional spring ($S_0=S_L=\infty$) at both ends, while Fig. 5 illustrates the frequencies of the FG NLSG rod with a hard spring ($S_0=\infty$) on one end and a soft spring ($S_L=0$) on the other. As the functionally gradient index enhances, the decrease in torsional frequencies of FG nano-sized rod can be easily seen. This decrease is valid for both Figures. As it is mentioned before, as the functionally gradient index value enhances, the metallic properties of the FG nanorod increase. The conclusion to be drawn from this is that the metallization of the mechanical properties of the FG NLSG rod causes a decrease in their frequency. That is, increasing functionally gradient index value has a softening impact on the FG NLSG rod.

Figs. (6)-(9) demonstrate the variation of torsional frequencies of FG NLSG rods for the various functionally

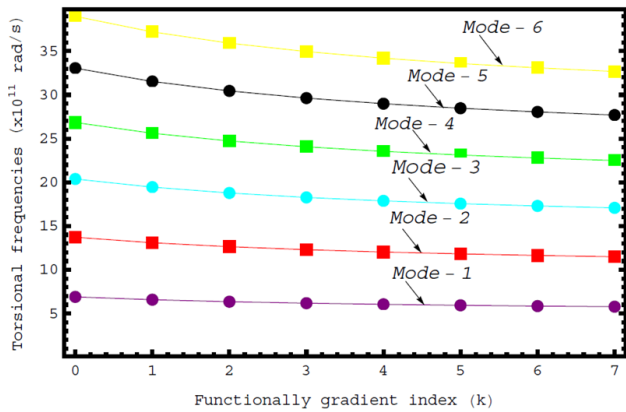


Fig. 4 Variation of torsional frequencies of FGM nanorod versus functionally gradient index ($S_0=S_L=\infty$, $\sqrt{\mu}=0.5$ nm, $l=0.3$ nm)

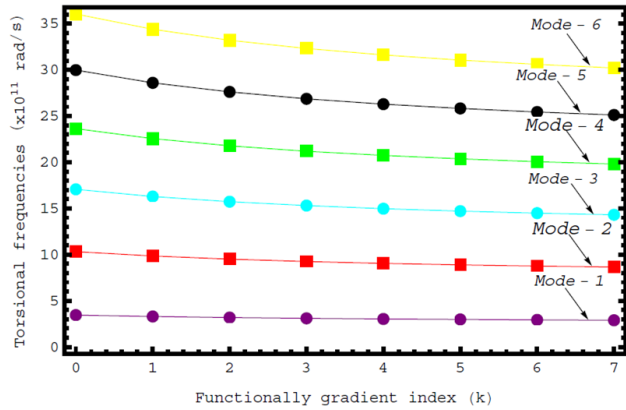


Fig. 5 Variation of torsional frequencies of FGM nanorod versus functionally gradient index ($S_0=\infty$, $S_L=\infty$, $\sqrt{\mu}=0.5$ nm, $l=0.3$ nm)

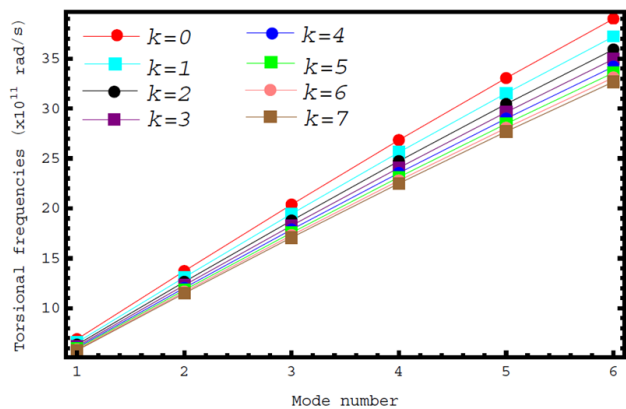


Fig. 6 Variation of torsional frequencies of FGM nanorod versus mode number ($S_0=\infty$, $S_L=\infty$, $\sqrt{\mu}=0.5$ nm, $l=0.3$ nm)

gradient index ($k=0, 1, 2, 3, 4, 5, 6, 7$) versus mode number. Figs. (6) and (7) show the variation of frequencies for FG nanorods with hard springs ($S_0= S_L=\infty$), while Figs. (8) and (9) illustrate the variation of frequencies for FG nanorods with hard-soft springs ($S_0= \infty$, $S_L=0$). The softening effect of the functionally graded index on radially FG nonlocal strain gradient rods is clearly visible from these Figures. It should also be noted here that at $k=0$ the frequencies of the

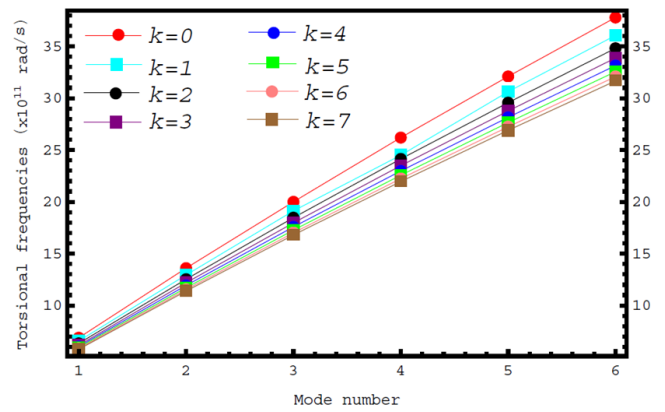


Fig. 7 Variation of torsional frequencies of FGM nanorod versus mode number ($S_0=\infty$, $S_L=\infty$, $\sqrt{\mu}=1.0$ nm, $l=0.8$ nm)

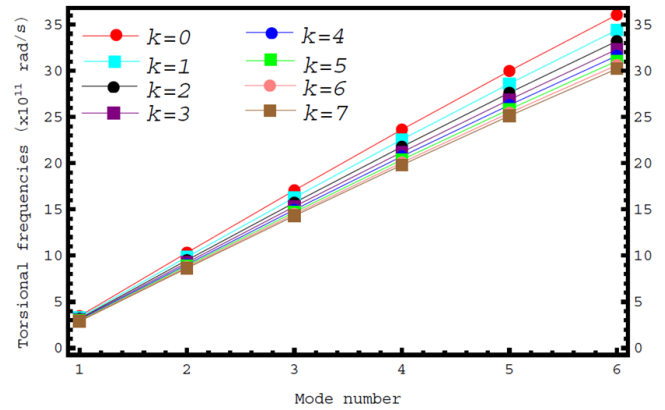


Fig. 8 Variation of torsional frequencies of FGM nanorod versus mode number ($S_0=\infty$, $S_L=0$, $\sqrt{\mu}=0.5$ nm, $l=0.3$ nm)

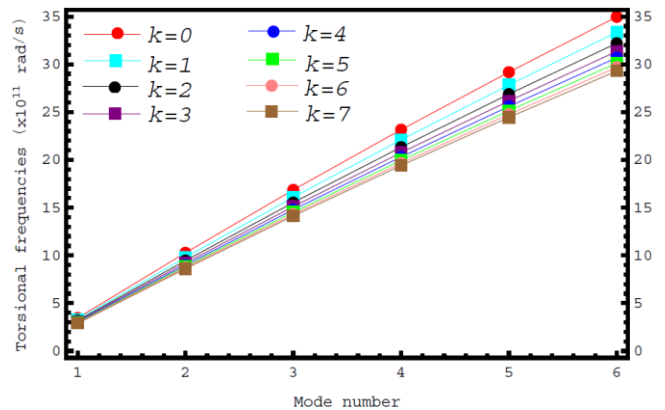


Fig. 9 Variation of torsional frequencies of FGM nanorod versus mode number ($S_0=\infty$, $S_L=0$, $\sqrt{\mu}=1.0$ nm, $l=0.8$ nm)

FG nano-sized rod are reduced to the frequencies of a ceramic nanorod. Another issue that draws attention in the Figs. is that the frequencies of the FG NLSG rod with hard torsional springs on both sides are higher than the frequencies of the FG NLSG rod with soft torsional springs on one side. This means that the frequencies increase with increasing spring stiffness.

As it is known, in this paper, small-scale dependent torsional vibration behavior based on NLSG theory, which is a combination of two different non-classical elasticity

Table 6 Torsional frequencies (10^{11} rad/s) of FG nanorods for various small-scale parameters (mode 1)

$\sqrt{\mu}$	l	functionally gradient index		
		$k=0$	$k=2$	$k=4$
0 nm	0 nm	6.91	6.37	6.06
0.5 nm	0.5 nm	6.91	6.37	6.06
1.0 nm	1.0 nm	6.91	6.37	6.06
0.5 nm	1.0 nm	6.97	6.43	6.12
0.5 nm	1.5 nm	7.08	6.52	6.21
0.5 nm	2.0 nm	7.22	6.65	6.33
1.0 nm	0.5 nm	6.85	6.31	6.00
1.5 nm	0.5 nm	6.75	6.22	5.92

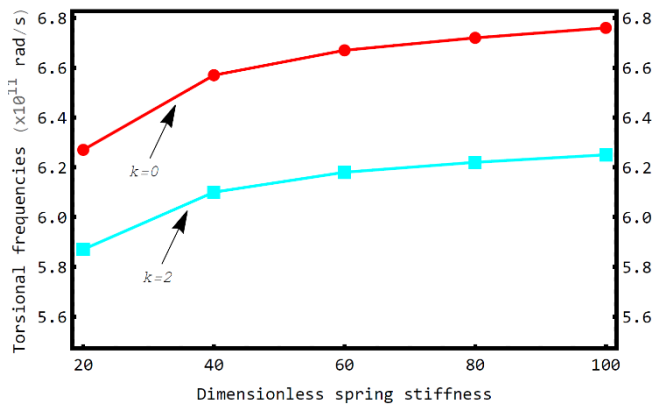


Fig. 10 Variation of torsional frequencies of FGM nanorod versus symmetrical dimensionless spring stiffness (mode 1, $\sqrt{\mu} = 0.5$ nm, $l=0.1$ nm)

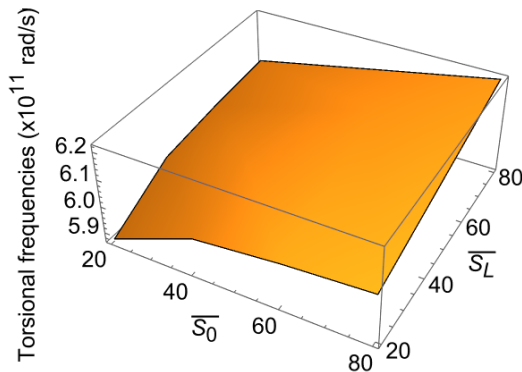


Fig. 11 Variation of torsional frequencies of FGM nanorod versus anti-symmetrical dimensionless spring stiffness (mode 1, $\sqrt{\mu} = 0.5$ nm, $l=0.1$ nm)

theories, is investigated. In this theory of elasticity, the effects of two different size parameters (μ and l) are reflected in the behavior together. Table 6 is given to compare the effects of these two small-scale parameters. For Table 6, three different functionally gradient index ($k=0, 2, 4$) are selected and $S_0=S_L=\infty$ is considered for the spring stiffnesses of the FG nanorod. In addition, small scale parameters are taken at various values from 0 nm to 2 nm. The softening effect of the functionally graded index is also clearly visible here. The main point to be emphasized here is the effect of size parameters $\sqrt{\mu}$ and l on torsional

vibration frequencies of radially functionally graded nanorod. As it is known, the frequency values obtained by neglecting both of the small scale parameters ($\sqrt{\mu} = 0$ nm and $l=0$ nm) belong to the classical theory of elasticity. The frequency values found by giving values $\sqrt{\mu} = l$ are given in the first three rows of Table 6. As can be seen, the frequency values in these three rows are equal to each other. This means that these two small scale parameters balance each other. That is, although both size parameters are included in the calculations, if these parameters are taken equal, the frequencies will be equal to the frequencies of the classical elasticity theory. Moreover, e_0 is taken constant and the solution is made with increasing values of l . As can be understood, an increase in l also causes an increase in torsional frequencies of radially functionally graded nanorod. This is due to the hardening effect of l . In addition, the torsional frequency values of FG nanorod obtained by keeping l constant and increasing values of $\sqrt{\mu}$ are written in the last two rows of Table 6. It can be understood from this that the increase in $\sqrt{\mu}$ causes a decrease in torsional frequencies. This is due to the softening effect of $\sqrt{\mu}$. To interpret a general conclusion from this, there is an increase in the frequency values when l is larger, while there is a decrease in the frequency values when $\sqrt{\mu}$ is larger. In other words, NLSG theory affects nanostructures as both a hardening and a softening.

In Fig. 10, the torsional frequency values of FG NLSG rods with equal stiffness at both ends are plotted. The aim here is to investigate the effect of spring parameters on vibration frequencies. In this example using 100-term, dimensionless spring stiffnesses $\bar{S}_0 = \bar{S}_L = 20, 40, 60, 80, 100$ are chosen. The increase in torsional frequencies with increasing $\bar{S}_0 = \bar{S}_L$ values can be easily observed. It is seen that the slope decreases as $\bar{S}_0 = \bar{S}_L$ values increase. This means that changes occurring at small $\bar{S}_0 = \bar{S}_L$ values affect the frequencies more.

Finally, figure 11 is drawn. In the previous example, the frequencies of FG NLSG rods with symmetrical spring stiffnesses are analyzed. In the model presented in this work, two different spring parameters are included in the solution and it is possible to assign different stiffnesses to these spring parameters. Figure 11 is presented to illustrate this efficiency. From the frequency values calculated considering $k=2$, it can be emphasized again that increasing spring stiffnesses cause an increase in frequencies. From this example, it is clear that we can control the vibration of the FG NLSG rod by changing only the spring stiffnesses attached to its ends without playing with its other properties. Although dimensionless spring stiffnesses 20-80 are considered in this example, it should be emphasized that countless stiffness combinations can be assigned.

6. Conclusions

There exist several studies on the application of the higher order elasticity theories to analyse the mechanical and dynamical behaviour of elastic nanobeams, nanorods and nanotubes with rigid support conditions. This study does not intend to provide a new analysis of non-deformable classical boundary conditions. Using a mathematical

process 'called Stokes' transformation, this work aims to give a Fourier sine series solution for free vibration and static analysis of FG nanorods subjected to different sets of deformable and rigid boundary conditions. The material properties of the nanorod vary in radius direction of circular section. Obtained results are validated with earlier research and studies. The effects of the different functionally gradient indexes, various deformable boundary conditions and various material scale parameters on the dynamical response of the functionally graded nanorod are investigated in detail.

References

- Akgöz, B. and Civalek, Ö. (2013), "A size-dependent shear deformation beam model based on the strain gradient elasticity theory", *Int. J. Eng. Sci.*, **70**, 1-14. <https://doi.org/10.1016/j.ijengsci.2013.04.004>
- Akgöz, B. and Civalek, Ö. (2014), "Thermo-mechanical buckling behavior of functionally graded microbeams embedded in elastic medium", *Int. J. Eng. Sci.*, **85**, 90-104. <https://doi.org/10.1016/j.ijengsci.2014.08.011>
- Alazwari, M.A., Esen, I., Abdelrahman, A.A., Abdraboh, A.M. and Eltaher, M.A. (2022), "Dynamic analysis of functionally graded (FG) nonlocal strain gradient nanobeams under thermo-magnetic fields and moving load", *Adv. Nano Res.*, **12**(3), 231-251. <https://doi.org/10.12989/anr.2022.12.3.231>
- Apuzzo, A., Barretta, R., Faghidian, S.A., Luciano, R. and De Sciarra, F.M. (2018), "Free vibrations of elastic beams by modified nonlocal strain gradient theory", *Int. J. Eng. Sci.*, **133**, 99-108. <https://doi.org/10.1016/j.ijengsci.2018.09.002>
- Arda, M. and Aydoğdu, M. (2021), "Dynamics of nonlocal strain gradient nanobeams with longitudinal magnetic field", *Math. Meth. Appl. Sci.*, **2021**, 1-18. <https://doi.org/10.1002/mma.7268>
- Barretta, R., Faghidian, S.A., De Sciarra, F.M. and Vaccaro, M.S. (2019), "Nonlocal strain gradient torsion of elastic beams: variational formulation and constitutive boundary conditions", *Arch. Appl. Mech.*, **90**(4), 691-706. <https://doi.org/10.1007/s00419-019-01634-w>
- Bohidar, S.K., Sharma, R. and Mishra, P.R. (2014), "Functionally Graded Materials: A Critical review", *Int. J. Res.*, **1**(7), 289-301.
- Çalım, F.F. (2019), "Vibration analysis of functionally graded Timoshenko beams on Winkler-Pasternak elastic foundation", *Iran J. Sci. Technol. Transact. Civil Eng.*, **44**(3), 901-920. <https://doi.org/10.1007/s40996-019-00283-x>
- Çalım, F.F. and Cuma, Y.C. (2021), "Forced vibration analysis of viscoelastic helical rods with varying cross-section and functionally graded material", *Mech. Based Des. Struct.*, **51**(7), 3620-3631. <https://doi.org/10.1080/15397734.2021.1931307>
- Civalek, O., Uzun, B. and Yaylı, M.O. (2022b), "A Fourier sine series solution of static and dynamic response of nano/micro-scaled FG rod under torsional effect", *Adv. Nano Res.*, **12**(5), 467-487. <https://doi.org/10.12989/anr.2022.12.5.467>
- Civalek, Ö., Uzun, B. and Yaylı, M.Ö. (2022a), "Torsional vibrations of functionally graded restrained nanotubes", *Eur. Phys. J. Plus*, **137**(1). <https://doi.org/10.1140/epjp/s13360-021-02309-8>
- Civalek, Ö., Uzun, B. and Yaylı, M.Ö. (2022c), "An effective analytical method for buckling solutions of a restrained FGM nonlocal beam", *Comput. Appl. Math.*, **41**(2). <https://doi.org/10.1007/s40314-022-01761-1>
- Civalek, Ö., Uzun, B., Yaylı, M.Ö. and Akgöz, B. (2020), "Size-dependent transverse and longitudinal vibrations of embedded carbon and silica carbide nanotubes by nonlocal finite element method", *Eur. Phys. J. Plus*, **135**(4). <https://doi.org/10.1140/epjp/s13360-020-00385-w>
- Devnath, I., Islam, M.N., Siddique, M.U.M. and Tounsi, A. (2022), "Static deflection of nonlocal Euler Bernoulli and Timoshenko beams by Castigliano's theorem", *Adv. Nano Res.*, **12**(2), 139-150. <https://doi.org/10.12989/anr.2022.12.2.139>
- Ding, H. and She, G. (2021), "A higher-order beam model for the snap-buckling analysis of FG pipes conveying fluid", *Struct. Eng. Mech.*, **80**(1), 63. <https://doi.org/10.12989/sem.2021.80.1.063>
- Dong, B., Li, H., Wang, X., Sun, W., Luo, Z., Ma, H., Qin, Z. and Han, Q. (2022), "Nonlinear forced vibration of hybrid fiber/graphene nanoplatelets/polymer composite sandwich cylindrical shells with hexagon honeycomb core", *Nonlinear Dyn.*, **110**(4), 3303-3331. <https://doi.org/10.1007/s11071-022-07811-x>
- Ebrahimi, F., Barati, M.R. and Civalek, Ö. (2019), "Application of Chebyshev-Ritz method for static stability and vibration analysis of nonlocal microstructure-dependent nanostructures", *Eng. Comput.*, **36**(3), 953-964. <https://doi.org/10.1007/s00366-019-00742-z>
- Ermiş, M. (2020), "Eksenel fonksiyonel derecelendirilmiş helislerin karşık sonlu eleman yöntemi ile serbest titreşim analizi", *Niğde Ömer Halisdemir Üniversitesi Mühendislik Bilimleri Dergisi*, **10**(1), 319-327. <https://doi.org/10.28948/ngumuh.823385>
- Ghandourah, E.E., Ahmed, H.M., Eltaher, M.A., Attia, M.A. and Abdraboh, A.M. (2021), "Free vibration of porous FG nonlocal modified couple nanobeams via a modified porosity model", *Adv. Nano Res.*, **11**(4), 405-422. <https://doi.org/10.12989/anr.2021.11.4.405>
- Gül, U. and Aydoğdu, M. (2021), "Transverse wave propagation analysis in single-walled and double-walled carbon nanotubes via higher-order doublet mechanics theory", *Waves Random Complex Med.*, **33**(3), 762-793. <https://doi.org/10.1080/17455030.2021.1959085>
- Hadji, L., Avcar, M. and Civalek, Ö. (2021), "An analytical solution for the free vibration of FG nanoplates", *J. Brazil. Soc. Mech. Sci. Eng.*, **43**(9). <https://doi.org/10.1007/s40430-021-03134-x>
- Jalaei, M., Thai, H. and Civalek, Ö. (2022), "On viscoelastic transient response of magnetically imperfect functionally graded nanobeams", *Int. J. Eng. Sci.*, **172**, 103629. <https://doi.org/10.1016/j.ijengsci.2022.103629>
- Khoram, M. M., Hosseini, M., Hadi, A. and Shishesaz, M. (2020), "Bending analysis of bidirectional FGM Timoshenko nanobeam subjected to mechanical and magnetic forces and resting on Winkler-Pasternak Foundation", *Int. J. Appl. Mech.*, **12**(8), 2050093. <https://doi.org/10.1142/s1758825120500933>
- Khosravi, F., Simyari, M., Hosseini, S.A. and Tounsi, A. (2020), "Size dependent axial free and forced vibration of carbon nanotube via different rod models", *Adv. Nano Res.*, **9**(3), 157-172. <https://doi.org/10.12989/anr.2020.9.3.157>
- Kiani, Y. and Eslami, M. R. (2010), "Thermal buckling analysis of functionally graded material beams", *Int. J. Mech. Mater. Des.*, **6**(3), 229-238. <https://doi.org/10.1007/s10999-010-9132-4>
- Koizumi, M. (1997), "FGM activities in Japan", *Compos. Part B Eng.*, **28**(1-2), 1-4. [https://doi.org/10.1016/s1359-8368\(96\)00016-9](https://doi.org/10.1016/s1359-8368(96)00016-9)
- Li, H., Dong, B., Zhao, J., Zou, Z., Zhao, S., Wang, Q., Han, Q. and Wang, X. (2022a), "Nonlinear free vibration of functionally graded fiber-reinforced composite hexagon honeycomb sandwich cylindrical shells", *Eng. Struct.*, **263**, 114372. <https://doi.org/10.1016/j.engstruct.2022.114372>
- Li, H., Li, Z., Xiao, Z., Xiong, J., Wang, X., Han, Q., Zhou, J. and Guan, Z. (2022b), "Vibro-impact response of FRP sandwich plates with a foam core reinforced by chopped fiber rods", *Compos. Part B Eng.*, **242**, 110077.

- <https://doi.org/10.1016/j.compositesb.2022.110077>
- Li, L. and Hu, Y. (2016), “Nonlinear bending and free vibration analyses of nonlocal strain gradient beams made of functionally graded material”, *Int. J. Eng. Sci.*, **107**, 77-97. <https://doi.org/10.1016/j.ijengsci.2016.07.011>
- Li, L., Hu, Y. and Li, X. (2016), “Longitudinal vibration of size-dependent rods via nonlocal strain gradient theory”, *Int. J. Mech. Sci.*, **115-116**, 135-144. <https://doi.org/10.1016/j.ijmecsci.2016.06.011>
- Li, X., Li, L., Hu, Y., Ding, Z. and Deng, W. (2017), “Bending, buckling and vibration of axially functionally graded beams based on nonlocal strain gradient theory”, *Compos. Struct.*, **165**, 250-265. <https://doi.org/10.1016/j.compstruct.2017.01.032>
- Lim, C., Zhang, G. and Reddy, J. N. (2015), “A higher-order nonlocal elasticity and strain gradient theory and its applications in wave propagation”, *J. Mech. Phys. Solids*, **78**, 298-313. <https://doi.org/10.1016/j.jmps.2015.02.001>
- Madenci, E. (2021), “Free vibration and static analyses of metal-ceramic FG beams via high-order variational MFEM”, *Steel Compos. Struct.*, **39**(5), 493. <https://doi.org/10.12989/scs.2021.39.5.493>
- Mahinzare, M., Amanpanah, S. and Ghadiri, M. (2021), “Size-Dependent higher order Thermo-Mechanical vibration analysis of two directional functionally graded material nanobeam”, *J. Solid Mech.*, **13**(1), 11-26. <https://doi.org/10.22034/jsm.2019.1866704.1427>
- Naebe, M. and Shirvanimoghaddam, K. (2016), “Functionally graded materials: A review of fabrication and properties”, *Appl. Mater. Today*, **5**, 223-245. <https://doi.org/10.1016/j.apmt.2016.10.001>
- Noroozi, R., Barati, A., Kazemi, A., Norouzi, S. and Hadi, A. (2020), “Torsional vibration analysis of bi-directional FG nanocone with arbitrary cross-section based on nonlocal strain gradient elasticity”, *Adv. Nano Res.*, **8**(1), 13. <https://doi.org/10.12989/anr.2020.8.1.013>
- Norouzzadeh, A., Ansari, R. and Rouhi, H. (2019), “An analytical study on wave propagation in functionally graded nanobeams/tubes based on the integral formulation of nonlocal elasticity”, *Waves Random Complex Med.*, **30**(3), 562-580. <https://doi.org/10.1080/17455030.2018.1543979>
- Numanoğlu, H.M., Ersoy, H., Akgöz, B. and Civalek, Ö. (2021), “A new eigenvalue problem solver for thermo-mechanical vibration of Timoshenko nanobeams by an innovative nonlocal finite element method”, *Math. Meth. Appl. Sci.*, **45**(5), 2592-2614. <https://doi.org/10.1002/mma.7942>
- Rahmani, A., Babaei, A. and Faroughi, S. (2020), “Vibration characteristics of functionally graded Micro-Beam carrying an attached mass”, *Mech. Adv. Compos. Struct.*, **7**(1), 49-58. <https://doi.org/10.22075/maacs.2019.18186.1214>
- Rao, S.S. (2019) *Vibration of Continuous Systems*, John Wiley & Sons, Hoboken, NJ, U.S.A.
- Sahmani, S. and Safaei, B. (2019), “Nonlinear free vibrations of bi-directional functionally graded micro/nano-beams including nonlocal stress and microstructural strain gradient size effects”, *Thin Wall. Struct.*, **140**, 342-356. <https://doi.org/10.1016/j.tws.2019.03.045>
- Setoodeh, A., Shahri, M.R.Z. and Rezaei, M.P. (2016), “Linear and nonlinear torsional free vibration of functionally graded micro/nano-tubes based on modified couple stress theory”, *Appl. Math. Mech.*, **37**(6), 725-740. <https://doi.org/10.1007/s10483-016-2085-6>
- Shahba, A. and Rajasekaran, S. (2012), “Free vibration and stability of tapered Euler-Bernoulli beams made of axially functionally graded materials”, *Appl. Math. Modell.*, **36**(7), 3094-3111. <https://doi.org/10.1016/j.apm.2011.09.073>
- Shakhlavi, S.J., Hosseini-Hashemi, S. and Nazemnezhad, R. (2020), “Torsional vibrations investigation of nonlinear nonlocal behavior in terms of functionally graded nanotubes”, *Int. J. Non-Linear Mech.*, **124**, 103513. <https://doi.org/10.1016/j.ijnonlinmec.2020.103513>
- Shen, Y., Chen, Y. and Li, L. (2016), “Torsion of a functionally graded material”, *Int. J. Eng. Sci.*, **109**, 14-28. <https://doi.org/10.1016/j.ijengsci.2016.09.003>
- Shi, X., Zuo, P., Zhong, R., Guo, C. and Wang, Q. (2022), “Vibration analysis of combined functionally graded cylindrical-conical shells coupled with annular plates in thermal environment”, *Compos. Struct.*, **294**, 115738. <https://doi.org/10.1016/j.compstruct.2022.115738>
- Timesli, A. (2021), “A cylindrical shell model for nonlocal buckling behavior of CNTs embedded in an elastic foundation under the simultaneous effects of magnetic field, temperature change, and number of walls”, *Adv. Nano Res.*, **11**(6), 581-593. <https://doi.org/10.12989/anr.2021.11.6.581>
- Tlidji, Y., Benferhat, R., Trinh, L.C., Tahar, H.D. and Abdelouahed, T. (2021), “New state-space approach to dynamic analysis of porous FG beam under different boundary conditions”, *Adv. Nano Res.*, **11**(4), 347-359. <https://doi.org/10.12989/.2021.11.4.347>
- Uzun, B. and Yaylı, M.Ö. (2020), “Nonlocal vibration analysis of Ti-6Al-4V/ZrO2 functionally graded nanobeam on elastic matrix”, *Arab. J. Geosci.*, **13**(4). <https://doi.org/10.1007/s12517-020-5168-4>
- Xu, X., Wang, X., Zheng, M. and Ma, Z. (2017), “Bending and buckling of nonlocal strain gradient elastic beams”, *Compos. Struct.*, **160**, 366-377. <https://doi.org/10.1016/j.compstruct.2016.10.038>
- Yaylı, M.Ö., Uzun, B. and Deliktaş, B. (2021), “Buckling analysis of restrained nanobeams using strain gradient elasticity”, *Waves Random Complex Med.*, **32**(6), 2960-2979. <https://doi.org/10.1080/17455030.2020.1871112>
- Zarezadeh, E., Hosseini, V. and Hadi, A. (2019), “Torsional vibration of functionally graded nano-rod under magnetic field supported by a generalized torsional foundation based on nonlocal elasticity theory”, *Mech. Based Des. Struct. Mach.*, **48**(4), 480-495. <https://doi.org/10.1080/15397734.2019.1642766>
- Zhang, X., Zheng, S. and Zhou, Y. (2019), “An effective approach for stochastic natural frequency analysis of circular beams with radially varying material inhomogeneities”, *Mater. Res. Express*, **6**(10), 105701. <https://doi.org/10.1088/2053-1591/ab361c>

AT